

# Influence of the thermal history and composition on the melting/solidification process in Sn-Ag-Cu solders

A. Rudajevová<sup>1\*</sup>, K. Dušek<sup>2</sup>

<sup>1</sup>Charles University, Faculty of Mathematics and Physics, Department of Condensed Matter Physics, Ke Karlovu 5, 121 16 Prague 2, Czech Republic

<sup>2</sup>Czech Technical University in Prague, Faculty of Electrical Engineering, Department of Electrotechnology, Technická 2, 166 27 Prague 6, Czech Republic

Received 24 October 2011, received in revised form 9 February 2012, accepted 3 April 2012

## Abstract

Presented work shows the results of DSC measurement for six Sn based solders. The alloys  $\text{Sn}_{96}\text{Ag}_4$ ,  $\text{Sn}_{99}\text{Cu}_1$ ,  $\text{Sn}_{97}\text{Cu}_3$ ,  $\text{Sn}_{96.5}\text{Ag}_3\text{Cu}_{0.5}$ ,  $\text{Sn}_{95.5}\text{Ag}_{3.8}\text{Cu}_{0.7}$  and  $\text{Sn}_{63}\text{Pb}_{37}$  were studied in the temperature range from room temperature up to 400 °C. The transformation temperatures for melting as well as for solidification were influenced by the composition and thermal history of the alloys. The thermal history was altered by changing the maximum thermal cycle temperature and the heating/cooling rate. It is shown that the rate of solidification is far larger than that of the melting. The solidification rate is not influenced by neither the composition nor the thermal history of the material. Analysis of these results is presented.

**Key words:** Sn alloys, phase transformations, undercooling solidification, DSC

## 1. Introduction

Solders based on Sn and Pb had long been the most popular solders for electronic assembly due to their low cost and superior properties. Due to the health and environmental concerns, used lead was forbidden and new near-eutectic or ternary Sn-based solder alloys were developed in order to replace the Sn-Pb based alloys. The most popular solders are Sn-Ag, Sn-Cu and Sn-Ag-Cu alloys. In all these alloys there are small additions of Ag and Cu elements, hence the physical and chemical properties are still determined by the body-centred tetragonal structure of pure Sn. All these alloys show the effect of under-cooling, which is a typical property of Sn. A decrease of the solidification temperature is typical for metals that crystallize in a lattice with lower symmetry [1], such as Sn, Ga, Bi, Pb or In. The under-cooling effect is connected with the difficulty of nucleating a solid phase in a liquid phase. The under-cooling in Sn-solders influences their structure, for example the Sn-dendrite size and the formation of primary phases such as  $\text{Ag}_3\text{Sn}$  and  $\text{Cu}_6\text{Sn}_5$  [2, 3], and thereby affect their mechanical properties.

The solder alloys are commonly used in an electronic assembly for a conductive connection of electronic components and printed circuit boards (PCBs). The determining process for the formation of the microstructure is the reflow process, i.e., when the solder is heated up to the melting temperature and then cooled. During this reflow process, the dissolution of board and component lead materials in the solder can occur [4]. Electronic interconnects are typical multi-component systems with interfaces between solders, the electronic components and PCBs. Each of these components influences the different thermal and mechanical properties of the solder joint and its solidification process. Different thermal conductivity of the components (PCBs, Cu lead or electrical parts) composes different temperature gradients in the solder joint during solidification. Thermal conductivities of Sn-Ag-Cu alloys between 210 and 220  $\text{W m}^{-1} \text{K}^{-1}$  were found by Kim et al. [5] at room temperature. The highest thermal conductivity in this multi-component joint has Cu ( $386 \text{ W m}^{-1} \text{K}^{-1}$ ), while the lowest thermal conductivity has one of the most commonly used PCB materials FR4 ( $0.2 \text{ W m}^{-1} \text{K}^{-1}$ ).

\*Corresponding author: tel.: +420 22191 1654; fax: +420 22491 1061; e-mail address: [rud@mag.mff.cuni.cz](mailto:rud@mag.mff.cuni.cz)

The nucleation process during solidification of the alloys is one of the essential factors that determine their texture and other characteristics. There are two theoretical approaches to this nucleation. In a homogeneous nucleation, the solid forms homogeneously from a liquid. This type is based on the relation between the solid-liquid interfacial energy and volume free energy. In heterogeneous nucleation, a new solid phase forms on a particle or surface which catalyzes the nucleation event. The quantification of the heterogeneous nucleation is more difficult than that of the homogeneous nucleation. This is due to the complexity of interactions between the nucleating molecules and the underlying surface. The heterogeneous nucleation rate is strongly dependent on the character of the surface. It is evident that the solidification of the solders in a multi-component electronic joint system takes place at very complex conditions because there are very different material properties in various parts of this system. Various thermal conductivities and thermal expansion characteristics [6] of the component influence the quality of the interface and therefore the quality and lifetime of the multi-component joint.

Since the solidification process of the solder is a determining process for quality and lifetime of the electrical joint, it is therefore very important to study the parameters that can influence this process. The aim of this work is to investigate the influence of the chemical composition and the thermal history of the alloys on the transformation temperatures and on the rate of the melting and solidification. In order to study these properties in  $\text{Sn}_{96}\text{Ag}_4$ ,  $\text{Sn}_{99}\text{Cu}_1$ ,  $\text{Sn}_{97}\text{Cu}_3$ ,  $\text{Sn}_{96.5}\text{Ag}_3\text{Cu}_{0.5}$ ,  $\text{Sn}_{95.5}\text{Ag}_{3.8}\text{Cu}_{0.7}$  and  $\text{Sn}_{63}\text{Pb}_{37}$  solders, the DSC method will be used in the temperature range from room temperature up to  $400^\circ\text{C}$ .

## 2. Experimental part

The temperature dependences of the heat flow were determined in a DSC Setaram instrument in the

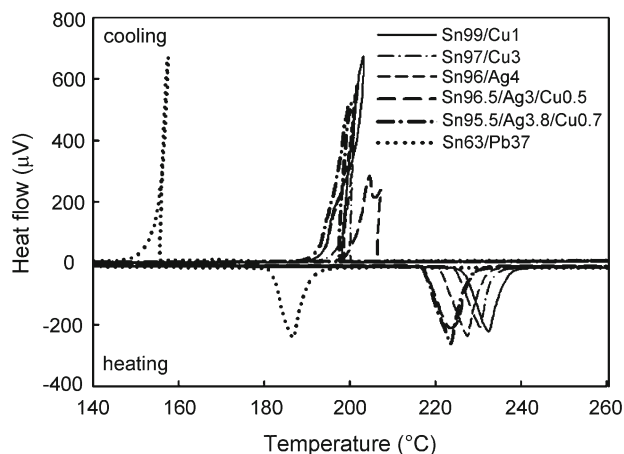


Fig. 1. Temperature dependence of the heat flow for  $\text{Sn}_{96}\text{Ag}_4$ ,  $\text{Sn}_{99}\text{Cu}_1$ ,  $\text{Sn}_{97}\text{Cu}_3$ ,  $\text{Sn}_{96.5}\text{Ag}_3\text{Cu}_{0.5}$ ,  $\text{Sn}_{95.5}\text{Ag}_{3.8}\text{Cu}_{0.7}$  and  $\text{Sn}_{63}\text{Pb}_{37}$  alloys.

temperature range of room temperature (RT) up to  $400^\circ\text{C}$ . The measurements were done under helium atmosphere. The heating/cooling rate was 2, 5, 7 and  $10\text{ K min}^{-1}$ . The sample was placed in an alumina crucible, and the transformation temperatures were determined as an onset of the transformation peaks.

The alloys  $\text{Sn}_{96}\text{Ag}_4$ ,  $\text{Sn}_{99}\text{Cu}_1$ ,  $\text{Sn}_{97}\text{Cu}_3$ ,  $\text{Sn}_{96.5}\text{Ag}_3\text{Cu}_{0.5}$ ,  $\text{Sn}_{95.5}\text{Ag}_{3.8}\text{Cu}_{0.7}$  and  $\text{Sn}_{63}\text{Pb}_{37}$  were commercially produced in Kovohutě Příbram and Cobar, and they were measured in the as-cast state. The  $\text{Sn}_{63}\text{Pb}_{37}$  alloy was used for comparison of the DSC results between this alloy and Pb free alloys. The presented results were obtained on the second and further runs to exclude the influence of the sample shape on the DSC results.

## 3. Results and discussion

Figure 1 shows DSC results for all materials studied. Numerical values of the transformation temperatures are presented in Table 1. It can be seen that all

Table 1. Transformation temperatures for Sn and Sn based alloys

Alloy	Temperature ( $^\circ\text{C}$ )		Hysteresis ( $^\circ\text{C}$ )
	melting	solidification	
$\text{Sn}_{96}\text{Ag}_4$	224.1	197.8	26.3
$\text{Sn}_{99}\text{Cu}_1$	223.4	200.5	22.9
$\text{Sn}_{97}\text{Cu}_3$	219.5	198.3	21.2
$\text{Sn}_{96.5}\text{Ag}_3\text{Cu}_{0.5}$	217.0	207.4	9.6
$\text{Sn}_{95.5}\text{Ag}_{3.8}\text{Cu}_{0.7}$	217.2	197.2	20
$\text{Sn}_{63}\text{Pb}_{37}$	183.0	154.9	28.1
Sn	231.2	200.2	31.0

Pb free solders have the melting points higher than the  $\text{Sn}_{63}\text{Pb}_{37}$  alloy and lower than the pure Sn. Hysteresis in the transformation temperatures was found for all solders. The largest hysteresis was found for pure Sn and the lowest for the  $\text{Sn}_{96.5}\text{Ag}_3\text{Cu}_{0.5}$  alloy. This alloy also shows two overlapping peaks during solidification. Similar results are presented by Song et al. [7] for the  $\text{SnAgIn}$  alloy. Their study of the microstructure has shown that during solidification In segregation leads to two kinds of solidification structures with different morphologies. The time dependence of the temperature measured by the thermocouple immersed in the molten solder has shown two maxima as well as in our DSC results. Except for this alloy, all Pb-free alloys show approximately the same solidification temperatures even though their melting points are different. Different melting points can be a consequence of the existence of various intermetallic particles in the solid alloys, which can act as nucleation centres (with different temperatures) for the melting process. The nucleation then takes place at various temperatures. In the liquid state  $\text{Sn}_{99}\text{Cu}_1$ ,  $\text{Sn}_{97}\text{Cu}_3$ ,  $\text{Sn}_{96}\text{Ag}_4$  and  $\text{Sn}_{95.5}\text{Ag}_{3.8}\text{Cu}_{0.7}$  alloys differ only by the small additions of Ag and Cu elements in Sn liquid, so small differences of the nucleation temperatures were found.

The shape of the transformation peaks (loops) during cooling is a consequence of the anomalous increase of the sample temperature at the transformation temperature range. A loop occurs when two values of the heat flow belong to one temperature. This occurs when the sample temperature during the phase transformation at first suddenly increases and immediately after that decreases. The temperature increase is a consequence of the release of latent heat. The time dependence of the thermocouple temperature measured below the sample during heating as well as during cooling is revealed in Fig. 2 (this data was obtained for  $\text{Sn}_3\text{Cu}$  at heating/cooling rate  $10\text{ K min}^{-1}$ ). We can see a difference in the character of these curves for heating and cooling. The sudden increase of the temperature during cooling is a consequence of the under-cooling.

The temperature measured by a thermocouple placed below the sample in the crucible is not the real temperature of the sample. This temperature is influenced by the thermal losses on the way from the sample to the thermocouple. An estimate of the difference between the real sample temperature and the temperature measured in DTA or DSC device can be made by a comparison of the temperature measured in this type of a device and the temperature measured by the immersed thermocouple. The results presented in the work of Zhao et al. [8] show that during the melting of Sn, the temperature in DTA or DSC is lower than in the sample by about  $2^\circ\text{C}$ . For the solidification process this difference may be as high as  $15^\circ\text{C}$ . Hence a question arises: What is the real temperat-

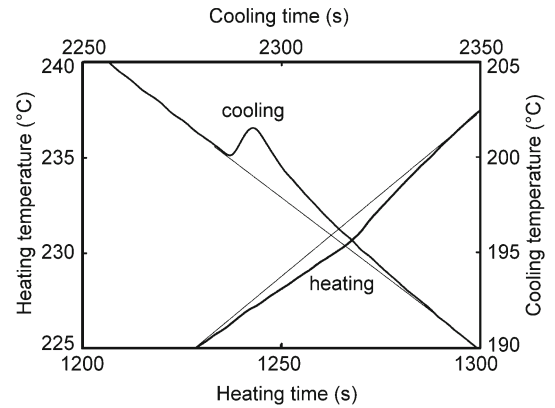


Fig. 2. The time dependence of the heating and cooling temperature for  $\text{Sn}_{96}\text{Ag}_4$  alloy.

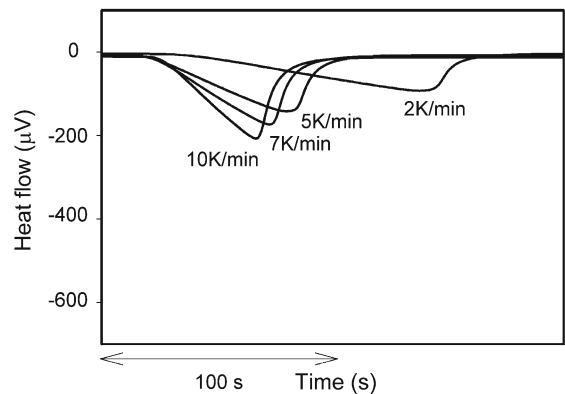


Fig. 3. The time dependence of the heat flow for heating of the  $\text{Sn}_{97}\text{Cu}_3$  alloy for the heating rates  $10\text{ K min}^{-1}$ ,  $7\text{ K min}^{-1}$ ,  $5\text{ K min}^{-1}$  and  $2\text{ K min}^{-1}$ .

ure of the sample in the transformation temperature range?

To answer this question, the time dependence of the heat flow was studied at various heating/cooling rates. These dependences are presented in Figs. 3 and 4. Both figures have the same scales of both axes. The curves are arranged so that the transformation processes start at the same place of the graph (not at the same time) to allow for an easy comparison of the characteristics of these dependences. Melting starts when the sample temperature spans the transformation temperature ( $T_{\text{TR}}$ ). If the sample is placed in the furnace, the transformation temperature is first reached on the sample surface. The phase interface with the transformation temperature propagates into the sample in the conduction range. When the transformation process continues during continued heating, the surface temperature becomes higher than  $T_{\text{TR}}$  while the temperature in the centre of the sample is still lower than  $T_{\text{TR}}$ . During the phase transformation,

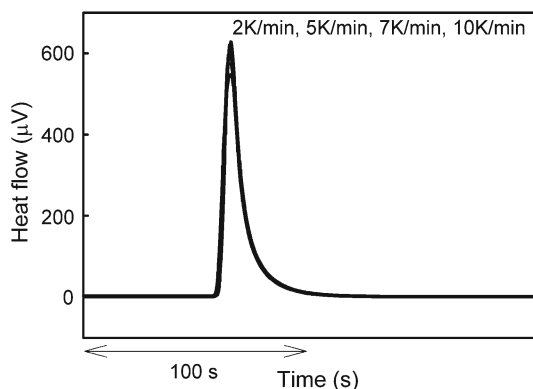


Fig. 4. The time dependence of the heat flow for cooling of the  $\text{Sn}_{97}\text{Cu}_3$  alloy for the cooling rates  $10 \text{ K min}^{-1}$ ,  $7 \text{ K min}^{-1}$ ,  $5 \text{ K min}^{-1}$  and  $2 \text{ K min}^{-1}$ .

the phase interface divides the sample into two parts with different temperature gradients (phases have different thermal conductivity). The interface velocity depends on the heating/cooling rate, the thermal conductivities and densities of both phases, and the latent heat [9]. All these parameters determine the sample temperature in a given place at a given time. The sample temperature is further influenced by the heat losses from the sample by heat conduction into the surrounding atmosphere, into the crucible, and also by radiation. It is evident that the temperature measured by the thermocouple below the sample in a crucible is not the real sample temperature and that this temperature has only informative character.

During solidification there is a different mechanism of the temperature changes than during melting. The cause of this behaviour is under-cooling. During cooling, the melted samples of the solder stay in the melted state at temperatures deep below the melting point. At a certain temperature, when nucleation occurs in the sample, solidification takes place practically immediately in a part of the sample, as can be seen in Fig. 4. The instant increase of the heat flow does not depend on the cooling rate (in our studied range of rates). A microscopy observation of the solidification of Pb-Sn alloys [10] confirms our results. The authors show that the rate of change of the advancing front decreases progressively from a large value at the beginning of the solidification. The initial rapid commencement of the phase transformation is connected with the release of latent heat and with heating of the sample (Fig. 4), leading to a reduction of the rate of the solidification. A smaller slope of dependences in Fig. 4 is given by the time lag of the temperature due to measurement of the temperature outside the sample. A similar departure is shown in [8] when the time dependence of the temperatures for the immersed thermocouple and the thermocouple below the sample is compared during solidification. The initial

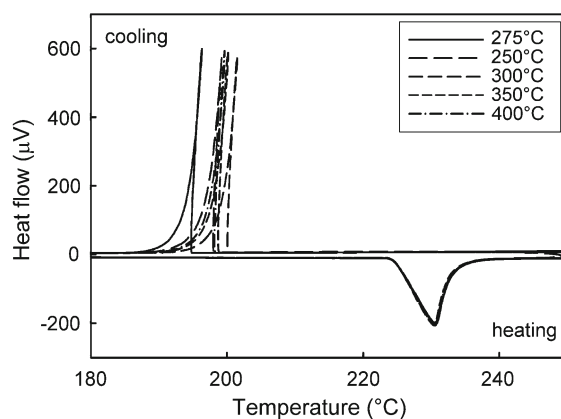


Fig. 5. The temperature dependence of the heat flow for  $\text{Sn}_{96}\text{Ag}_4$  at different maximum thermal cycle temperatures.

phase of the solidification leads to a steep increase of the sample temperature. This increase can be measured only with a fine thermocouple immersed in the melt. A study of the solidification of 163.2 mg of Sn [8] that was cooled by  $5 \text{ K min}^{-1}$  with immersed thermocouple shows that after nucleation and rapid initial dendritic growth the sample temperature increases by about  $27^\circ\text{C}$ . This process takes place only in a part of the sample in cooperation with heat conduction. In the first phase of the solidification a large temperature gradient occurs in the sample (tens of degrees). Under-cooling causes that the reverse phase transformation takes place in a shorter time and therefore the maximum temperature increase is larger than the maximum temperature decrease during melting.

It has been mentioned that solidification determines the physical properties of an electrical connection. A high rate in the solidification process is not advantageous for the quality of the connection due to the evolution of internal strain and non-equilibrium structures. The influence of the thermal history of the alloy on the under-cooling was studied by changing the maximum thermal cycle temperature and the heating/cooling rates. Figure 5 shows that the value of the maximum thermal cycle temperature influences the start temperature only for the solidification but not for the melting. It can be seen that this influence is rather random. The influence of the maximum thermal cycle temperature on the thermal hysteresis of pure Sn was studied by Kano [1]. In this work it was found that hysteresis increased with increasing maximum thermal cycle temperature until a certain limit was reached. The extent of changes of the solidification temperature upon changes of the maximum thermal cycle was practically the same as in our work. It was empirically found that there was a correlation between the maximum cycle temperature and the nucleation temperature [11]. This dependence was explained by a solid-like structure in the liquid. Those structures

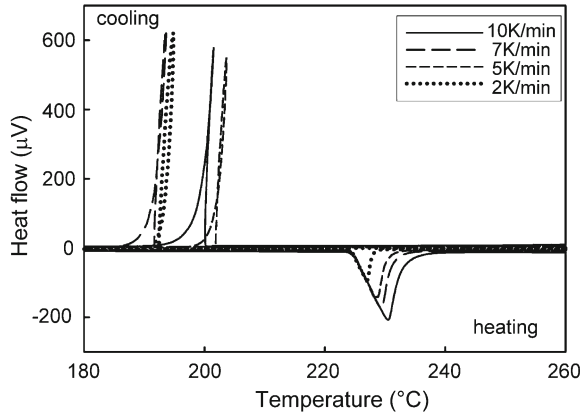


Fig. 6. Influence of the heating/cooling rates on the transformation temperatures for  $\text{Sn}_{96}\text{Ag}_4$  alloy.

were found in the liquids by X-ray measurements [12] or neutron diffraction [13] in the temperature range just above the melting point. It was shown that if some solid-like structure remained in the liquid above the melting point, it first vanished during heating of the melt up to a certain temperature. During the following cooling these changes persisted and influenced the nucleation temperature of the solidification. The influence of the maximum cycle temperature on the solidification process can also be a consequence of the concentration of inhomogeneities in the melt. Experimental studies of various systems in the liquid state show that at temperatures much higher than the melting point large concentration of inhomogeneities exists in the melt [14]. Arrangement of these inhomogeneities depends on the temperature and can also influence the nucleation process.

The influence of the heating-cooling rates on the solidification temperature is shown in Fig. 6 for the  $\text{Sn}_{97}\text{Cu}_3$  alloy. It can be seen that while the melting point is practically unaffected, the solidification temperature changes with the heating/cooling rate. The character of these changes is random. The difference between the highest and the lowest solidification temperature is about  $10^\circ\text{C}$ . If we compare the results from Fig. 3 and the results described in this paragraph, we can see that the heating/cooling rate influences the solidification temperature but not the velocity of the phase transformation.

The further effect that was observed in our study was ageing. DSC results measured in the first thermal cycle after casting of the alloy were different from those in the second thermal cycle. While the melting temperature was practically the same for both cycles, the solidification temperature in the first run was at about  $5^\circ\text{C}$  higher than in the second thermal cycle. If the same sample was measured after one month, nearly the same differences between two following thermal cycles were found. Only immediate re-

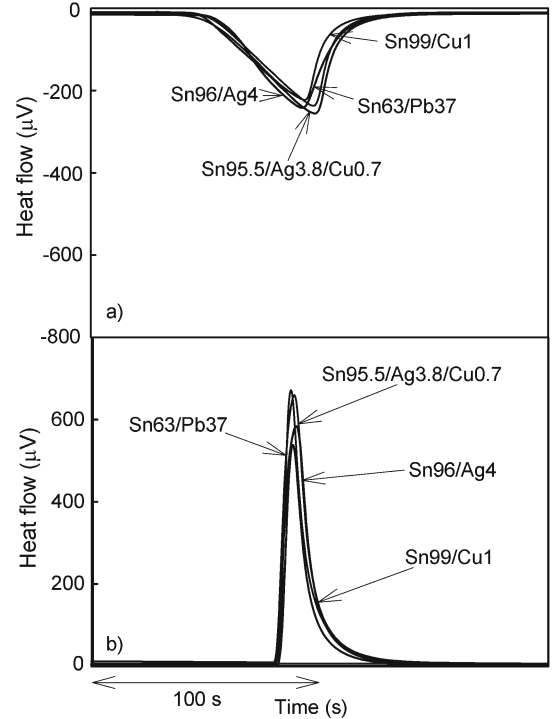


Fig. 7. Dependence of the heat flow on time for all studied alloys at  $10\text{ K min}^{-1}$  during a) heating and b) cooling.

peating of the measurement gave the same results. All these results show that while the nucleation temperature depends on the thermal history, the crystalline growth takes place with very high velocity that cannot be influenced by any parameter in our experiments.

The influence of the composition on the transformation temperatures is shown in Fig. 1. The influence of the composition on the transformation rate is revealed in Fig. 7 for the  $\text{Sn}_{96}\text{Ag}_4$ ,  $\text{Sn}_{99}\text{Cu}_1$ ,  $\text{Sn}_{95.5}\text{Ag}_{3.8}\text{Cu}_{0.7}$  and  $\text{Sn}_{63}\text{Pb}_{37}$  alloys. The composition has no influence on the transformation rates for melting and solidification. For the propagation of the melting front in the conduction region, the following relation was derived [9]:

$$-\lambda_L \left( \frac{\partial T}{\partial x} \right)_L = u\rho H - \lambda_S \left( \frac{\partial T}{\partial x} \right)_S, \quad (1)$$

where  $-\lambda_L \left( \frac{\partial T}{\partial x} \right)_L$  is heat flux in the liquid at the interface,  $u\rho H$  is the latent heat absorption rate, where  $u$  is the interface velocity,  $\rho$  is the density (it is assumed that the densities in both phases are the same) and  $H$  is the latent heat per unit mass. The last term  $-\lambda_S \left( \frac{\partial T}{\partial x} \right)_S$  describes the heat conducted away from the moving interface into the solid. The interface velocity  $u$  and temperature are time dependent. We can assume only a small difference in the density and the

latent heat (Fig. 1) for our Sn-Ag-Cu based alloys. In Kim et al. the work of [5], it was found that the thermal diffusivity of various Sn-Ag-Cu based alloys differs only marginally. It may be assumed that similar differences in the thermal diffusivity exist even for the liquid phases. The use of Eq. (1) for alloys with similar physical properties can lead to values close to the velocities of the interface movement during melting. This is in agreement with the results in Fig. 7a. For the solidification this progress cannot be used due to under-cooling.

#### 4. Conclusion

We can conclude that all Pb free Sn-Ag-Cu based alloys show similar behaviour. Sn<sub>96.5</sub>Ag<sub>3</sub>Cu<sub>0.5</sub> alloy differs by its two steps of solidification from all used alloys. While the melting point temperatures depend on the composition, the solidification temperatures are nearly the same for all studied alloys except for the Sn<sub>63</sub>Pb<sub>37</sub> alloy. Solid alloys contain different kinds and amounts of intermetallic phases, which cause nucleation centres at different temperatures. Liquid alloys are diluted solutions of Ag and Cu in Sn with a small difference in the concentration. The nucleation probably starts on the crucible wall for all alloys, and thus there is no concentration dependence. Solidification temperatures for all studied alloys depend on the thermal history, i.e. the maximum thermal cycle temperatures and the heating/cooling rates. Solidification takes place practically immediately in a large part of the sample. The rate of this process does not depend on the composition or the thermal history of material.

Temperature gradients during the solder alloy solidification may have an influence on the internal structure of the solder joint. Solidification depends on the used combination of materials (solder alloy, PCB, components) and the used cooling technology. The difference in the temperature gradient may also be caused by the different thermal masses of PCB and the other components.

#### Acknowledgements

This work is a part of the research programmes MSM 0021620834 and MSM No.6840770021 that are financed by the Ministry of Education of the Czech Republic.

#### References

- [1] Kano, M.: *Netsu Sokutei*, 18, 1991, p. 64.
- [2] Kang, S. K., Choi, W. K., Shih, D. Y., Henderson, D. W., Gosselin, T., Sarkhel, A., Goldsmith, C., Puttlitz, K. J.: *JOM*, 55, 2003, p. 61.  
[doi:10.1007/s11837-003-0143-6](https://doi.org/10.1007/s11837-003-0143-6)
- [3] Lehman, L. P., Athavale, S. N., Fullem, T. Z., Giamis, R. K., Kinyanjui, R. K., Lowenstein, M., Mather, K., Patel, R., Rae, D., Wang, J., Xing, Y., Zavalij, L., Borgesin, P., Cotts, E. J.: *J. Electron. Mater.*, 33, 2004, p. 1429. [doi:10.1007/s11664-004-0083-0](https://doi.org/10.1007/s11664-004-0083-0)
- [4] Handwerker, C., Kattner, U., Moon, K.: *Fundamental Properties of Pb-Free Solder Alloys, Lead-Free Soldering*. New York, Springer US 2007.
- [5] Kim, S. W., Lee, J., Jeon, B. M., Jung, E., Lee, S. H., Kang, K. H., Lim, K. T.: *Int. J. Thermophys.*, 30, 2009, p. 1234. [doi:10.1007/s10765-009-0603-5](https://doi.org/10.1007/s10765-009-0603-5)
- [6] Han, B., Guo, Y.: *Components, Packaging, and Manufacturing Technology, Part A*, IEEE Transactions, 19, 1996, p. 240. [doi:10.1109/95.506110](https://doi.org/10.1109/95.506110)
- [7] Song, J. M., Wu, Z. M., Huang, D. A.: *Scripta Mater.*, 56, 2007, p. 413. [doi:10.1016/j.scriptamat.2006.10.044](https://doi.org/10.1016/j.scriptamat.2006.10.044)
- [8] Zhao, J. C.: *Methods for Phase Diagram Determination*. Amsterdam, Elsevier 2007.
- [9] Gebhart, B.: *Heat Conduction and Mass Diffusion*. New York, McGraw-Hill, Inc. 1993.
- [10] Yoshioka, H., Tada, Y., Kunimina, K., Furuichi, T., Hayashi, Y.: *Acta Mater.*, 54, 2006, p. 757. [doi:10.1016/j.actamat.2005.09.038](https://doi.org/10.1016/j.actamat.2005.09.038)
- [11] Radochenko, I. B.: *Bunshi Butsurigaku II*. Tokyo, Sougou Kagaku Shuppan 1967.
- [12] Isherwood, R. S., Orton, B. R.: *Phil. Mag.*, 17, 1968, p. 561. [doi:10.1080/14786436808217743](https://doi.org/10.1080/14786436808217743)
- [13] Sarrah, P. C., Smith, G. P.: *J. Chem. Phys.*, 2, 1953, p. 228. [doi:10.1063/1.1698864](https://doi.org/10.1063/1.1698864)
- [14] Kalashnikov, E. V.: *Tech. Phys.*, 42, 1997, p. 430. [doi:10.1134/1.1258703](https://doi.org/10.1134/1.1258703)